Desalination 615 (2025) 119291

Contents lists available at ScienceDirect

Desalination

journal homepage: www.elsevier.com/locate/desal

Brackish water vs. brine outfall: impact of desalination plant discharge in vulnerable coastal sites

Francesca De Serio [a,b,*], Diana De Padova [a,b], Giancarlo Chiaia [a], Mouldi Ben Meftah [a,b], Michele Mossa [a,b]

[a] *Polytechnic University of Bari, DICATECh, Via E. Orabona 4, 70125 Bari, Italy*
[b] *CoNISMa – Inter University Consortium for Marine Sciences, Piazzale Flaminio 9, 00196 Rome, Italy*

HIGHLIGHTS

- The assessment of brackish water effluent discharge as an alternative to conventional brine outfall is considered
- Numerical modeling reveals key differences in hydrodynamics and plume patterns induced by hypo- and hypersaline discharges.
- Indicators of plume spreading show that hypersaline discharge tends to increase stagnation in enclosed inlet
- The method provides insights into sustainable desalination in vulnerable coastal sites

GRAPHICAL ABSTRACT

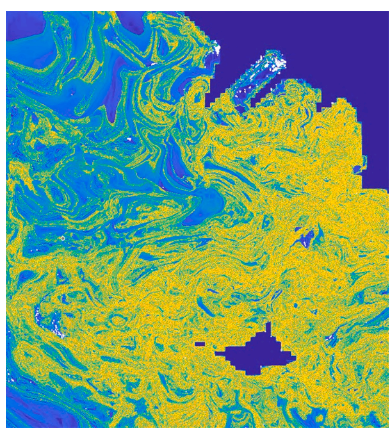

ARTICLE INFO

Keywords:
Desalination
Brackish discharge
Hypersaline plume
Diffusivity
Timescale
Coastal impact

ABSTRACT

The potential of coastal springs has recently been explored as an alternative water source for desalination plants. Unlike conventional seawater-fed facilities, this approach produces a brackish effluent. Our study aims to investigate the environmental implications of the discharge of such brackish water from a planned desalination facility in a vulnerable coastal area of Southern Italy. We employ numerical modeling of hydrodynamics and plume dispersion to compare two scenarios: (1) discharge of hyposaline brackish water, as envisaged by the proposed approach; and (2) discharge of hypersaline brine, as in traditional plants. Year-long simulations reveal key differences between the two scenarios. We introduce and discuss two relevant metrics for assessing plume impacts: the eddy diffusivity, which quantifies mixing efficiency, and the characteristic time scale, which links plume length scale to ambient current speed. Our main findings highlight (i) how differences in plume density alter local hydrodynamics; (ii) the extent to which plume spreading time and length scales differ, with consequent variation in potential ecosystem impacts. Results suggest that brackish effluent management could represent a more sustainable alternative for coastal desalination, minimizing environmental risks. In contrast,

* Corresponding author at: Polytechnic University of Bari DICATECh, Via E. Orabona 4, 70125 Bari, Italy.
E-mail address: francesca.deserio@poliba.it (F. De Serio).

https://doi.org/10.1016/j.desal.2025.119291
Received 4 March 2025; Received in revised form 16 July 2025; Accepted 7 August 2025
Available online 9 August 2025

hypersaline plumes may require offshore release to reduce ecological impact. Although this study is region-specific, the proposed framework is applicable to other coastal areas facing similar desalination challenges.

1. Introduction

Freshwater scarcity is a critical challenge in many regions, particularly in areas with limited natural water resources and growing demands due to urbanization and climate change. This is expected because of factors such as longer periods of droughts, excessive freshwater withdrawal, seawater intrusion with salinization of coastal aquifers, all amidst rising global population, living standards and industrialization. Soni et al. [1] report that approximately 66 % of the global population encounters water shortage for a minimum of one month annually. To tackle freshwater shortage, the last decades witnessed an exponential increase of desalination plants installed worldwide, reaching more than 19,000 plants in 2020 [2]. At present, seawater desalination represents a viable solution to bridge the growing gap between natural freshwater availability and demand, with a global production rate of 99 million cubic meters per day [3]. Moreover, as a limitless and climate-independent resource, it enhances clean water availability in coastal areas with scarce or overused supplies. It is recognized as essential for achieving the United Nations' Sustainable Development Goal 6 on sustainable water management and sanitation [4].

The growing reliance on desalination as a solution to supplement traditional water supplies has raised concerns about the environmental impacts of waste discharges on ecosystems. Among various disposal methods for desalination concentrate (such as deep-well injection, evaporation ponds, and treatment at wastewater facilities), sea brine disposal remains the most cost-effective option. However, discharging concentrate into the sea creates a dense hypersaline plume that sinks and spreads along the seabed, altering the physical and chemical properties of receiving waters. This can degrade water quality, affect local fisheries, and harm benthic marine organisms adapted to stable salinity environments [5]. To mitigate these impacts, the design of desalination plants and outfalls must consider the physical, chemical, and biological characteristics of the local marine environment. Thorough preliminary research, which includes assessments of marine circulation, wave conditions, and water quality, is crucial. Mathematical modeling is often used to predict the effects of brine discharge and optimize outfall design, ensuring minimal environmental harm while meeting water demands [6–8]. Site-specific factors such as bathymetry, currents, and temperature influence the extent of damage, making advanced design methodologies essential. Proper planning and the use of advanced design methodologies are essential to minimize potential harm. For instance, the use of submarine pipelines equipped with diffusers for brine discharge is a well-established practice. Thus, one challenge for the desalination industry is to develop new water resources without increasing pressure on the marine environment [9]. The other is to provide a significant environmental advantage also in terms of groundwater conservation.

Recently, efforts have been made to explore alternative sources, including the utilization of coastal springs with relatively low salinity levels that require only minimal desalination. This alternative to seawater intake offers several benefits. It avoids critical issues such as marine shells clogging intake structures, seasonal water currents and tides bringing suspended matter that complicate filtration, dust storms fertilizing coastal waters leading to algal blooms, and the persistent problem of membrane fouling. Additionally, the wastewater discharged after desalination has a very low salinity content, offering multiple environmental benefits: reduction of environmental stress by minimizing the impact on marine organisms and benthic habitats; improved ecosystem health and biodiversity as it avoids altering the natural salinity gradient critical for coastal ecosystems; higher dilution capacity. This novel approach thus aligns well with sustainable marine management goals [4].

The present paper focuses on the case study of the Taranto municipality in southern Italy (Fig. 1) located along the Ionian Sea, in Puglia

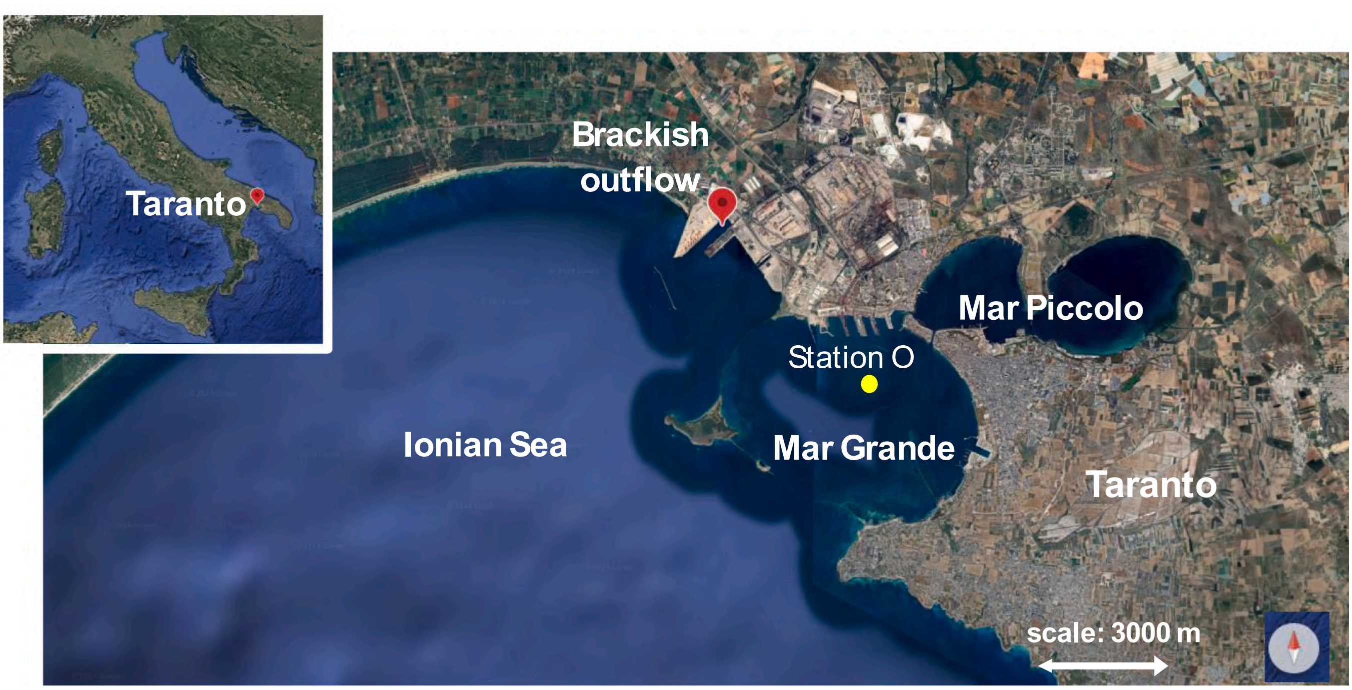

Fig. 1. Target area showing the location of the brackish water outflow (17.164° E, 40.505° N) and the meteo-oceanographic monitoring station (Station O, 17.127° E, 40.277° N). Source: Google Earth.

region, where some coastal springs have been identified as a key potential source for a novel desalination plant, especially due to sufficient capacity, existing infrastructure, and strategic location near major water distribution networks. This realization could alleviate the pressure on existing aquifers, improve the resilience of the region's water supply system, reduce the risk of environmental degradation associated with excessive groundwater extraction and align with the protection measures outlined in the Regional Technical Regulations of the Water Protection Plan [10].

The present study aims at evaluating the environmental implications of discharging desalinated brackish water into the neighbouring coastal area, considering that the balance between the need for alternative water sources and the protection of coastal and marine ecosystems requires sustainable water management practices. In fact, the coastal area of Taranto is a valuable yet delicate resource, impacted by both natural changes and human activities. It experiences substantial pollution from heavy industry and military shipyards [11–13] that poses significant ecological risks to marine life and human health [11,14]. Despite being subject to urban and industrial waste as well as heavy naval traffic, the hydrogeological features of Taranto's coast have supported a diverse range of transitional habitats and high biodiversity [15].

Considering that coastal managers require simple, transferable metrics to gauge ecological risk, here we define two such indicators: the horizontal eddy diffusivity, which quantifies lateral mixing efficiency, and the characteristic time scale, which links the plume's spatial extent to the ambient current speed. These metrics enable direct comparison across sites and support threshold-based decision making. Thus, our findings are expected to contribute to broader discussions on the integration of desalination in regions facing similar water scarcity challenges, especially in the Mediterranean, while highlighting the importance of minimizing the environmental footprint of such interventions and also to increase awareness on the necessity of regional adaptation strategies.

2. Regional context and target site description

Despite the existing hydraulic infrastructure network across the entire region providing a certain management flexibility for water distribution, Puglia remains an area historically prone to water crises. Analyses of the volumes stored in its four main reservoirs have shown an increasingly frequent occurrence of critical hydrological years over the last thirty years. A significant factor contributing to this phenomenon is ongoing climate change, which undoubtedly negatively affects the reservoirs' capacity to recharge. This is compounded by a growing demand for water resources due to increasing anthropic pressure. In recent years, the main artificial reservoirs that supply Puglia have recorded filling levels well below their maximum storage capacities. Today's water scenario in Puglia, therefore, sees its main source of supply, the large reservoirs, increasingly in crisis, leading to excessive exploitation of the aquifer system. Of the total 17,000 l/s, almost 25 % comes from groundwater extraction, whose reserves are already overexploited for irrigation purposes.

In summary, the geographic features of Puglia, which naturally lack permanent watercourses and abundant groundwater systems, suggest that a promising solution could be the potential use of coastal springs, which have lower salinity levels and require less intensive desalination than seawater, making them ideal for providing additional water volumes with limited environmental impact. Tara Spring stands out as the most suitable option. With a usable flowrate of 400 l/s from its main spring, it is the most abundant in the region [16]. Historically used for irrigation, it already has existing capture and lifting infrastructures, which would reduce the costs associated with the necessary works. Additionally, the use of the Tara spring for irrigation has significantly decreased in recent years, leaving a substantial portion of the resource available for other uses, such as potable water. Moreover, the Tara spring is located near a strategic infrastructure hub for the supply of the entire southern part of the region.

The proposed desalination plant treating water from the Tara River should have the following main features. The water should be extracted near the existing intake facility, utilizing submerged electric pumps installed within the intake channel of the Tara River springs. The water quality has been assessed based on the parameter limits set by Italian Legislative Decree 31/2001, which governs water intended for human consumption. Monitoring actions conducted by regional authorities identified exceedances only for parameters related to salinity, namely hardness, electrical conductivity, sodium, and chloride. Pollutants of clear anthropogenic origin, such as nitrates, fluorides, hexavalent chromium, and vanadium, were consistently found at concentrations below the drinking water limits [17]. To meet the plant's needs, the current flow rate from the Tara spring will be augmented by incorporating contributions from the available secondary springs, allowing the total expected flow rate to reach 1000 l/s. It is estimated that at full capacity, the plant could produce approximately 19.87 million m^3 yearly. The plant features parallel processing lines based on Ultrafiltration and Reverse Osmosis (RO). All feedwater undergoes ultrafiltration, with the RO permeate being remineralized using a blend of post-ultrafiltration water. The expected recovery rate of the plant is approximately 70 %, resulting in the production of 680 l/s of potable water for the city and 320 l/s of waste. It would be discharged by gravity into the sea in the port area. The salinity of the brackish discharge is expected to be 7 psu (practical salinity unit), compared to an average ambient salinity of 38.5 psu in the discharge area. Regarding other physicochemical characteristics, the discharged water is anticipated to comply with the standards set by Italian Legislative Decree 152/2006, as amended. The proposed discharge location in this study is situated within the port area, specifically in a narrow inlet. While this setting may appear disadvantageous (since it constrains plume dispersion and limits dilution) it was recommended by regional authorities for technical and economic reasons, as it enables the use of existing conduits. The geographical coordinates of the site are 17.164° E, 40.505° N, as shown in Fig. 1.

3. Methods: Numerical model and implemented runs

The numerical simulations have been executed by using the numerical model MIKE 3FM distributed by the Danish Hydraulic Institute [18]. The model, largely used in coastal hydrodynamics and oceanography, solves the three-dimensional time-dependent conservation equations of momentum and mass, adopting the explicit finite difference method. Current velocities and thermohaline data necessary for its implementation have been derived from the products of CMEMS (Copernicus Marine Environment Service. Specifically, data have been extracted from the Mediterranean Sea Physics Reanalysis dataset [19] having horizontal grid resolution of 1/24° (~ 4.2 km) and 72 unevenly spaced vertical levels (i.e. the MEDSEA_ ANALYSIS_ FORECAST_PHY_006_013 database has been adopted). The atmospheric data, time- and space-varying, used as initial and boundary condition are wind velocity [m/s], atmosphere pressure [Pa], total cloud cover [%], solar radiation [J/m^{-2}], air temperature [°C]). They have been extracted by ERA5 dataset developed through the Copernicus Climate Change Service [12]. The turbulent closure model adopted in the MIKE 3FM model relies on the k-ε formulation for the vertical direction [20] and the Smagorinsky formulation for the horizontal plane [21].

The model had already been applied in numerous previous studies, utilizing field measurements [6,13,22]. In particular, based on sensitivity analyses conducted for the year 2020 in the Mediterranean domain [15], we performed the present simulation using the calibration parameters derived from those analyses: a seabed roughness of 0.1 m, a wind drag coefficient of 0.02, and a constant Smagorinsky coefficient of 0.6 [13]. As detailed in the results' section, the model validation has been carried out using salinity (S) data collected in the Mar Grande basin (Fig. 1) through a meteo-oceanographic station installed and managed

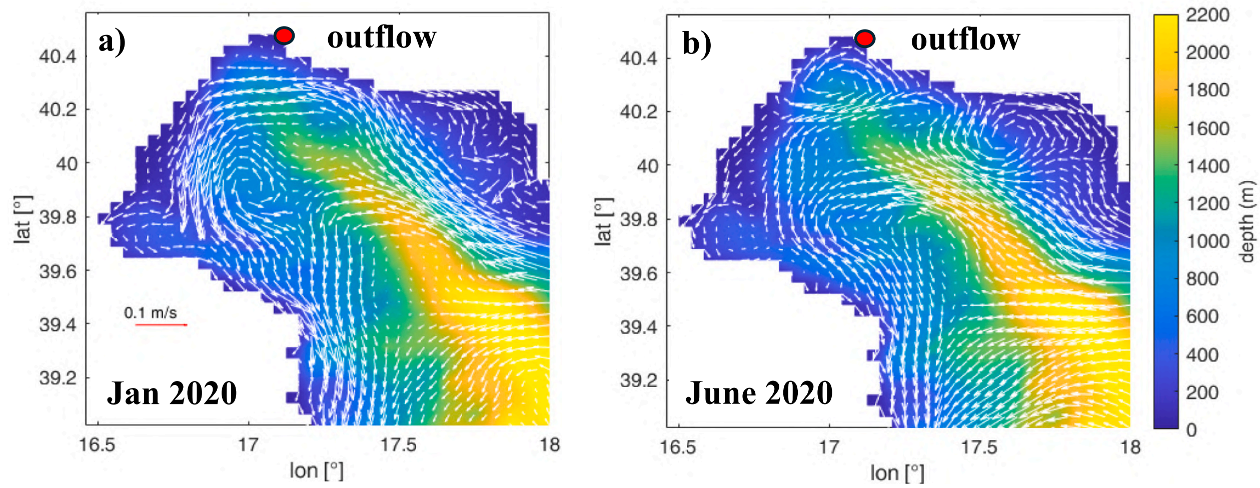

Fig. 2. CMEMS monthly-averaged superface currents: a) January 2020, b) June 2020. The red dot indicates the location of the outflow (17.164°E, 40.505°N). Same scale for velocity vectors in both panels. (For interpretation of the references to colour in this figure legend, the reader is referred to the web version of this article.)

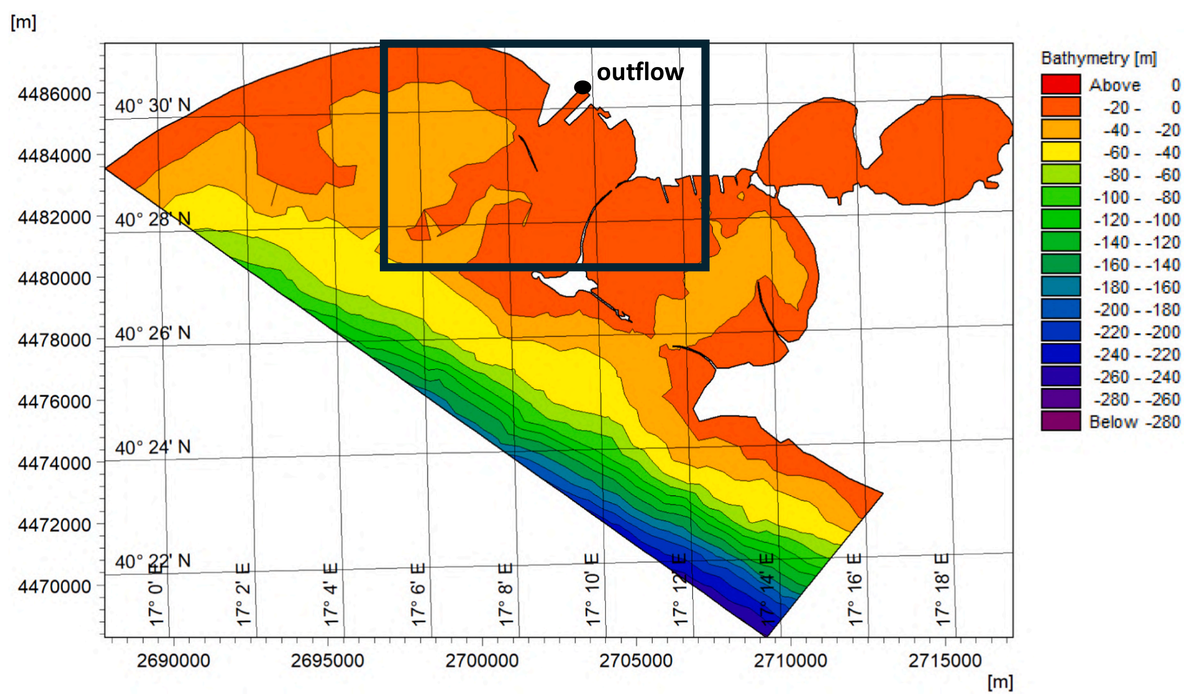

Fig. 3. Domain for the MIKE 3FM model application, with location of the outflow. The box indicates the area that is zoomed in for the simulation results in the following section. Gauss Boaga and geographycal coordinate systems shown.

by the LIC (Laboratory of Coastal Engineering) research unit at the Polytechnic University of Bari. A detailed description of this station is available in previous research by the same authors [11,12,23].

Fig. 2 shows, as an example, the monthly-averaged surface currents for January 2020 and June 2020, derived from CMEMS data. This selected domain covers a portion of the Ionian Sea that significantly exceeds our target site. This is because the available CMEMS data, characterized by a relatively coarse spatial resolution, are suited for describing processes at a regional scale. In this way, they result informative, revealing some typical and recurring hydrodynamic structures. For instance, in January, the coastal circulation is anticlockwise, with an anticlockwise gyre forming in the northwest part of the Ionian Sea and two less intense clockwise gyres forming along the northern (our target area) and northeast coasts, respectively. In June, the overall circulation remains predominantly anticlockwise along the deeper bathymetric contours. Along the northern and northeastern coasts, two clockwise gyres persist, while the anticlockwise gyre in the northwestern part of the area weakens. This regional information is particularly useful for defining the background scenario for our numerical simulations. However, to account for processes occurring at much finer spatial scales, as required in our case, the CMEMS data, acquired over the broader Ionian domain, have been used as input and boundary conditions to force the MIKE 3FM model on a smaller domain (Fig. 3), featuring a typical spatial resolution ranging from 50 to 100 m (local scale).

As previously mentioned, two different discharge conditions have been considered, applying the same annual meteomarine, hydrodynamic, and thermohaline forcings to the selected domain. The desalinated discharge flow rate was set at 320 l/s at the outfall point, with geographical coordinates 17.164° E, 40.505° N (or analogously 2,703,368 m E and 4,485,969 m N in Gauss-Boaga coordinates). The

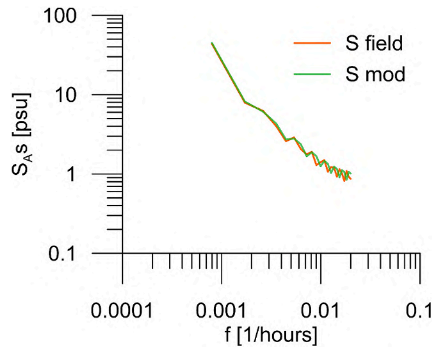

Fig. 4. Comparison of the amplitude spectra of salinity measured at Mar Grande station and salinity output from the model (Test S0) over a selected period (February 15 – April 30).

only difference between scenarios is the salinity of the discharged flow. This is because, given the brackish nature of the hypothesized discharge, local authorities have proposed releasing the effluent at the surface, treating it similarly to a river discharge, in order to take advantage of existing infrastructure.

Nonetheless, we conducted dedicated numerical simulations to evaluate the viability of this configuration, under two salinity scenarios. In Test LS (low salinity), the outflow salinity was set at 7 psu, representing the novel desalination plant concept. In Test HS (high salinity), the salinity was set at 50 psu, a value higher than that of the receiving body, as typically occurs in conventional desalination plants. Moreover, for each case, we considered two configurations: surface discharge, as suggested by the authorities, and bottom discharge at a depth of 11.3 m, corresponding to the local seabed. Therefore, four simulations were conducted: bottom discharge (Tests LS1 and HS1) and surface discharge (Tests LS2 and HS2).

Another discharge is present in the inlet, originating from the cooling system of a big industrial complex. Although historically significant, its flow rate has been drastically reduced in recent years due to decreased production. As this discharge could contribute to plume dilution, it was deliberately excluded from our simulations in order to consider the most conservative and potentially critical scenario.

According to national guidelines (Legislative Decree 152/2006), salinity increases from brine discharge must not exceed 5 % above ambient seawater salinity within a 50 m radius of the outfall. To meet this requirement, best practice recommends a submarine pipeline with a diffuser to enhance mixing and dilution, since a point-source hypersaline release could otherwise be non-compliant. We nevertheless included Tests HS1 and HS2 as reference cases, to compare directly with the brackish scenarios and to represent possible plant malfunctions. The results (see Results section) confirm that even these point-source releases satisfy the regulatory constraint on average. Howeve, to explore further mitigation options, we also simulated Test HS3, in which the hypersaline plume is released far offshore, at bottom, via a submarine pipe and diffuser. While this configuration is not part of the initial planning considerations, this scenario helps assess the benefits of discharge in a less confined, higher-current environment.

4. Results

4.1. Numerical model validation

As written in section 3, the model has been validated by using data measured in year 2020 by the meteo-oceanographic station in Mar Grande (Fig. 1). Among the different measured parameters, the station

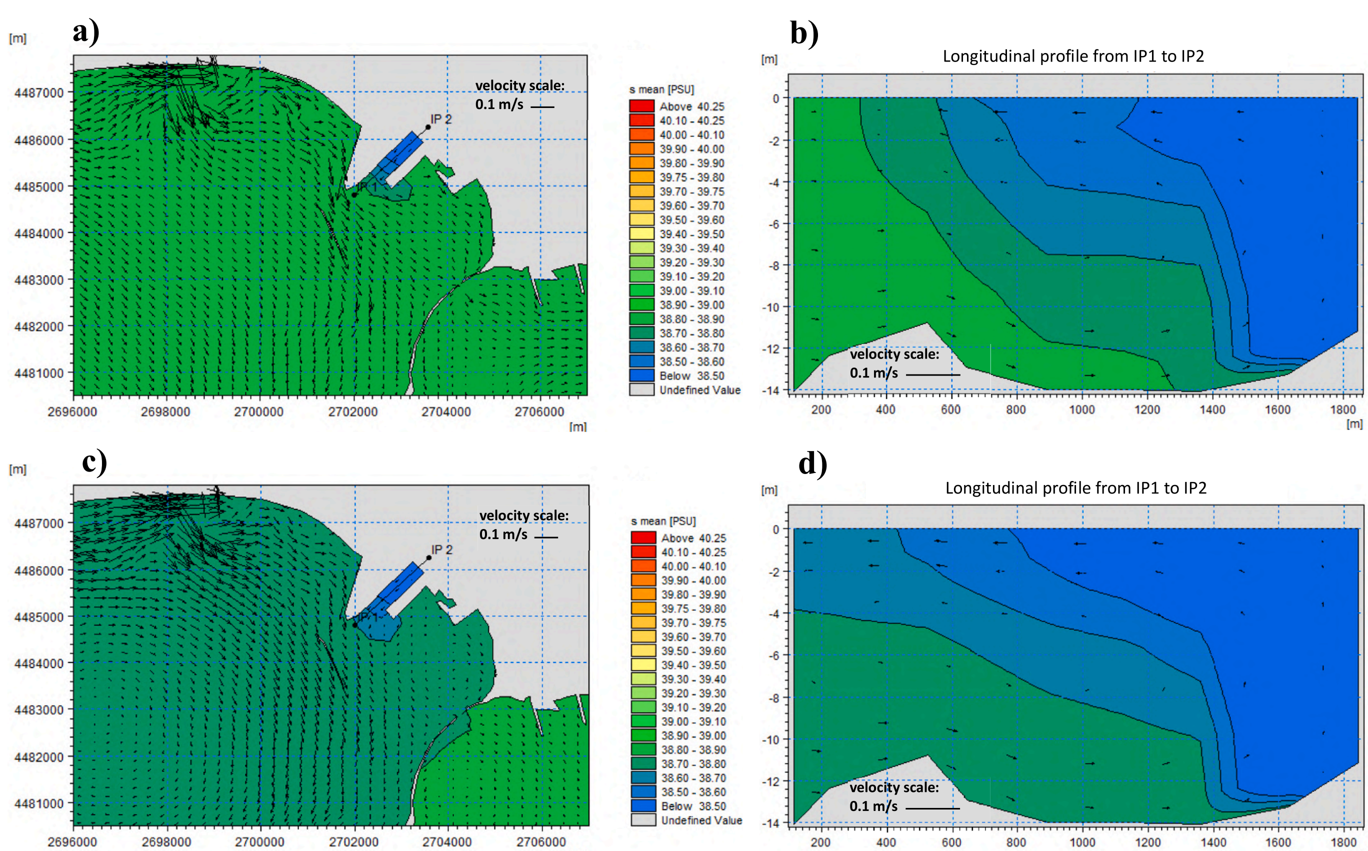

Fig. 5. Test LS1, time-averaged velocity maps. Left column: horizontal surface layer; Gaus Boaga Coordinates. Right column: selected vertical section along the inlet (IP1 – IP2). Top row: winter season; Bottom row: summer season.

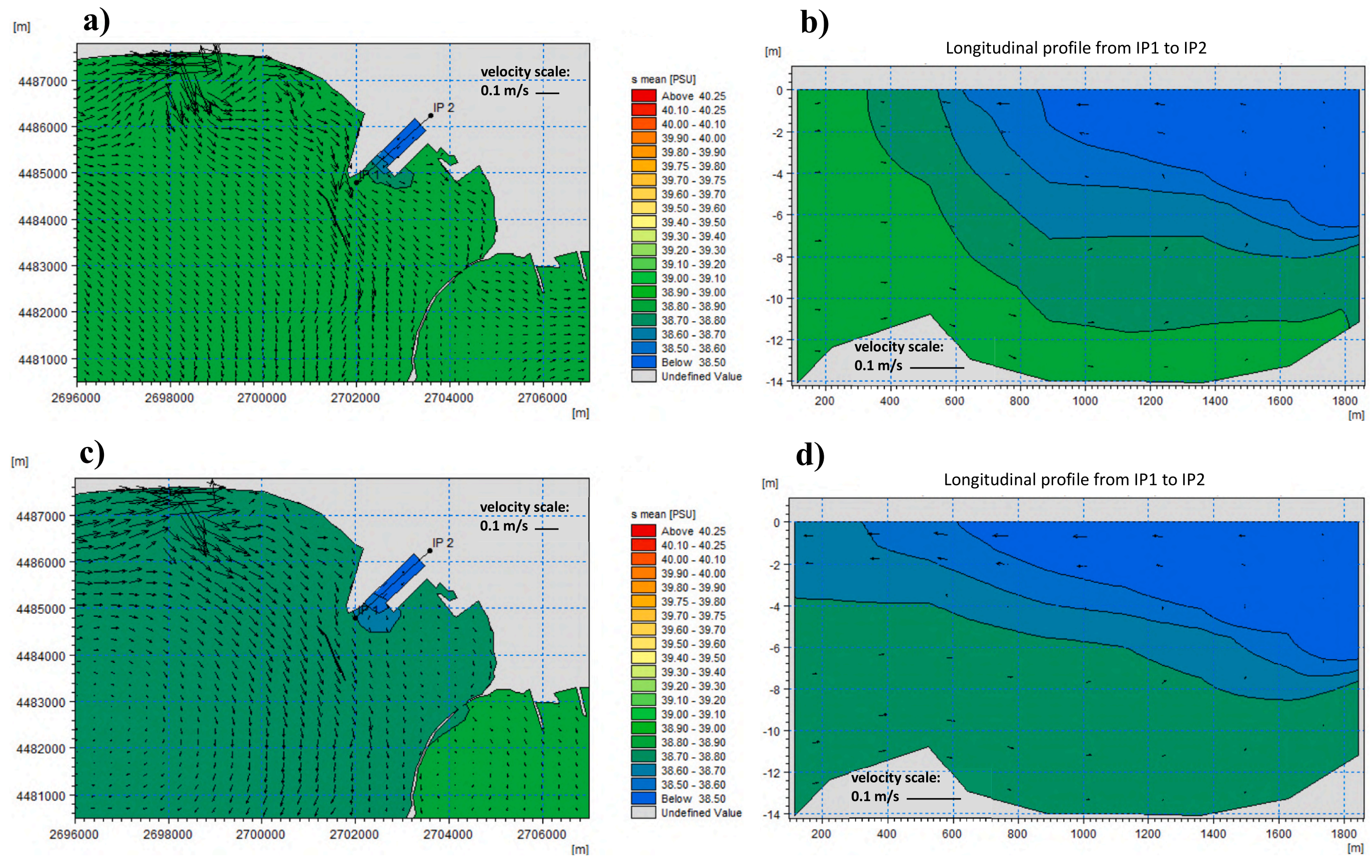

Fig. 6. Test LS2, time-averaged velocity maps. Left column: horizontal surface layer; Gaus Boaga Coordinates. Right column: selected vertical section along the inlet (IP1 – IP2). Top row: winter season; Bottom row: summer season.

also collected salinity (S) data by means of a CTD probe, located at 2.5 m from the sea surface, with a sampling frequency of one hour [11,12]. Based on the necessity to have a complete and continuous salinity time series for the analysis, an additional validation test of the MIKE 3FM model has been carried out for a selected period (i. e. February 15 – April 30), considering the actual real conditions, namely in the absence of any plant discharge (Test S0). The salinity parameter has been focused on, as in our case we particularly aim at describing the advection and mixing process of the plant discharge. The obtained statistics reveal a good agreement between measured S and S modelled at the same depth, providing a relative error of 2 % for the mean value and of 2.2 % for the *rms* (root mean square) value. Carrying out the validation also in the frequency domain, we have computed the amplitude spectra for salinity, both field and modelled ones, as shown in Fig. 4. They show a very satisfactory matching as for amplitudes and for frequency, especially at greater time scale, that is in the range (one month - one week), so capturing the main features of salinity variations in the long term.

4.2. Inlet release: Hydrodynamics and plume spreading

The results of Test LS1 and Test LS2 clearly show that the plume, discharged throughout the simulated year with a salinity of 7 psu, is positively buoyant. Particularly for Test LS1, once released at the bottom, it tends to rise to the surface, acting as a destabilizing buoyancy flux for the local vertical density distribution [24]. As a result, plume dispersion and dilution occur largely at the surface, for both Test LS1 and Test LS2, driving the circulation in the inlet and specifically inducing a surface flow directed offshore. This flow inhibits the entry of the branch of the clockwise gyre established in the northern area of the domain. Conversely, near the bottom, the same branch is not prevented from entering the inlet. Thus, an anticlockwise circulation cell forms along the longitudinal section of the inlet. This behavior is consistently observed during both winter and summer periods.

As an example, Fig. 5 for Test LS1 and Fig. 6 for Test LS2 illustrate these trends, showing salinity maps overlaid with velocity vectors for the average winter and summer conditions. For each seasonal condition, these figures display a zoomed view of the results at the surface in the horizontal plane (panels a, c) and in the longitudinal section (panels b, d) along the inlet P1-P2, as specified in the horizontal map.

It is evident that in Test LS1, the higher vertical mixing during winter, along with the more homogeneous distribution of temperature and salinity throughout the water column, leads to a more uniform vertical plume mixing (Fig. 5b) compared to the summer period (Fig. 5d). When the plume is released at the surface (Test LS2), the lower salinity concentration remains more confined to the upper layer near the release point and gradually spreads along the inlet without affecting the entire water column. In the longitudinal section of the inlet, within the first 400 m from the outflow point, the plume's behavior is similar under both winter and summer conditions for both Test LS1 and Test LS2. However, at greater distances, the vertical salinity gradient is smoother in summer than in winter. In summer, lower salinity remains more confined to the upper half of the water column due to stronger summer stratification. This effect is even more pronounced in Test LS2.

Fig. 7 and Fig. 8 display the seasonal average salinity maps and velocity vectors for Test HS1 and Test HS2 (analogous to Figs. 5 and 6), respectively. In contras to both Test LS1 and Test LS2, in Test HS, the hypersaline plume (discharged with a salinity of 50 psu) is evidently negatively buoyant. As a result, it tends to remain confined to the bottom where it was released in Test HS1 (Fig. 7) and sinks toward the bottom in Test HS2 (Fig. 8), consistently acting as a stabilizing buoyancy flux for the local vertical density distribution. Consequently, the hydrodynamics in the inlet, driven by the discharge, is characterized by an

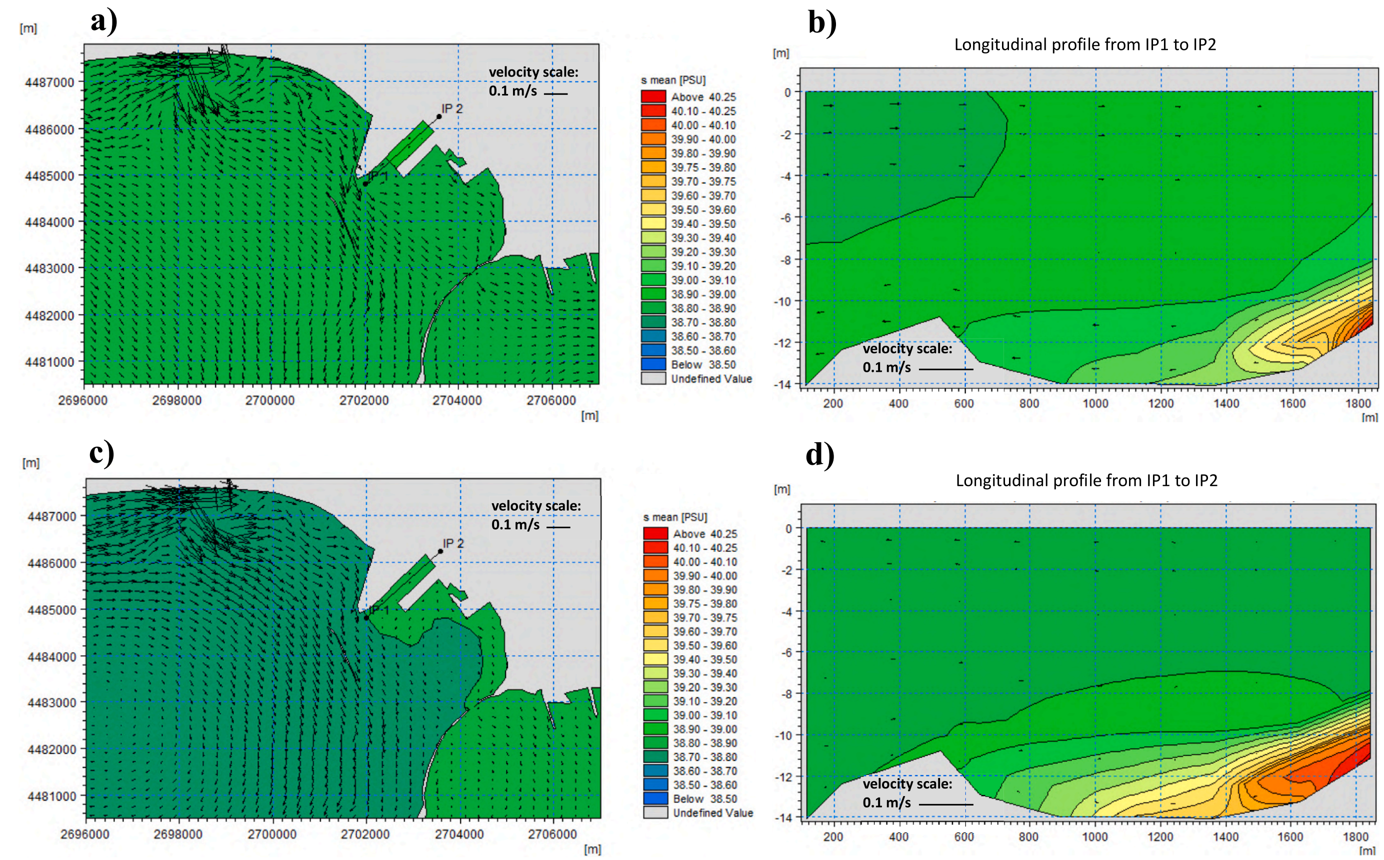

Fig. 7. Test HS1, time-averaged velocity maps. Left column: horizontal surface layer; Gaus Boaga Coordinates. Right column: selected vertical section along the inlet (IP1 – IP2). Top row: winter season; Bottom row: summer season.

outflow at the bottom, while at the surface the flow primarily enters the inlet. A resulting clockwise circulation arises in the longitudinal section of the inlet, especially evident in the winter period (Fig. 7b and Fig. 8b), while in summer, the circulation appears extermely weak on average (Fig. 7d and Fig. 8d). As previously noted, under Legislative Decree 152/2006, salinity must not exceed ambient seawater levels by more than 5 % within a 50 m radius of the discharge point. A hypersaline plume discharged at 50 psu from a single point, whether at the surface or near the seabed, might therefore appear counterproductive or potentially non-compliant. In our study, however, the legally permitted maximum salinity is 40.43 psu (i.e., 5 % above the average seawater salinity of 38.5 psu). On average, this threshold is never exceeded in either Test HS1 or Test HS2, as measured values consistently remain below the limit (see Figs. 7b,d and 8b,d).

Notably, the two LS scenarios, particularly Test LS1, result in slightly higher current velocities than the HS cases, both at the surface and bottom (as seen in the comparison between Figs. 5b, d, 6b, d, and Figs. 7b, d, 8b, d). In summer, the HS tests exhibit the weakest currents at both the surface and bottom (Figs. 7d and 8d). Thus, in terms of current magnitude, brine discharge has a much stronger impact in summer, reinforcing seasonal stratification and further inhibiting local circulation (Fig. 7d). This leads to more stagnant conditions, making the inlet a potential hotspot requiring careful management.

4.3. Inlet release: Dispersion time and length scales

For all tests, the numerical model outputs have been further processed and analyzed within the inlet. Based on and extending Taylor's theory of particle dispersion in the Eulerian framework [25,26], the annual time series of horizontal plane velocity, $u_H(t)$, at each point along the longitudinal axis of the inlet, was used to compute the autocorrelation function R_{UH}. Subsequently, the integral of the autocorrelation function up to the first zero-crossing was assessed, providing the so-called macro timescale τ_H [26–28]. This metric is highly informative as it gives a rough measure of the time taken by a fluid particle to become decorrelated from its initial state, thus representing the temporal scale of the largest eddies and thus serves as a useful ecological indicator.

As an example, Fig. 9 displays the autocorrelation function of surface and bottom velocity at a selected point in the inlet (i.e., the midpoint of the IP1-IP2 longitudinal axis) for all tests. At this location, the surface timescales are 42 h for Test LS1, 37 h for Test LS2, 50 h for Test HS1, and 25 h for Test HS2. At the bottom, the resulting timescales are 32 h for Test LS1, 38 h for Test LS2, approximately 11 days for Test HS1, and 40 h for Test HS2.

This result is significant as it further indicates that, in contrast to the LS scenarios, the HS scenario leads to a more stagnant condition especially at the bottom, with the hydrodynamics characterized by large, slowly circulating coherent structures. This condition is even more pronounced when the hypersaline plume is directly released at the bottom (Test HS1). This tendency is evidently unfavorable for the dispersion of the hypersaline plume. Conversely, in the case of the hyposaline plume, large eddies promote more rapid mixing at both surface and bottom, enhancing a more efficient transport of tracers and ensuring a more rapid renewal of water within the inlet. In terms of the release depth, it is evident that only in the case of the surface discharge of the hyposaline plume (Test LS2) the dispersion remains largely confined to the surface layer. In contrast, for all other scenarios, the dispersion extends to the bottom as well. This aspect is particularly significant when considering the preservation of specific ecological species that inhabit benthic habitats.

As previously stated, the adopted numerical model uses the

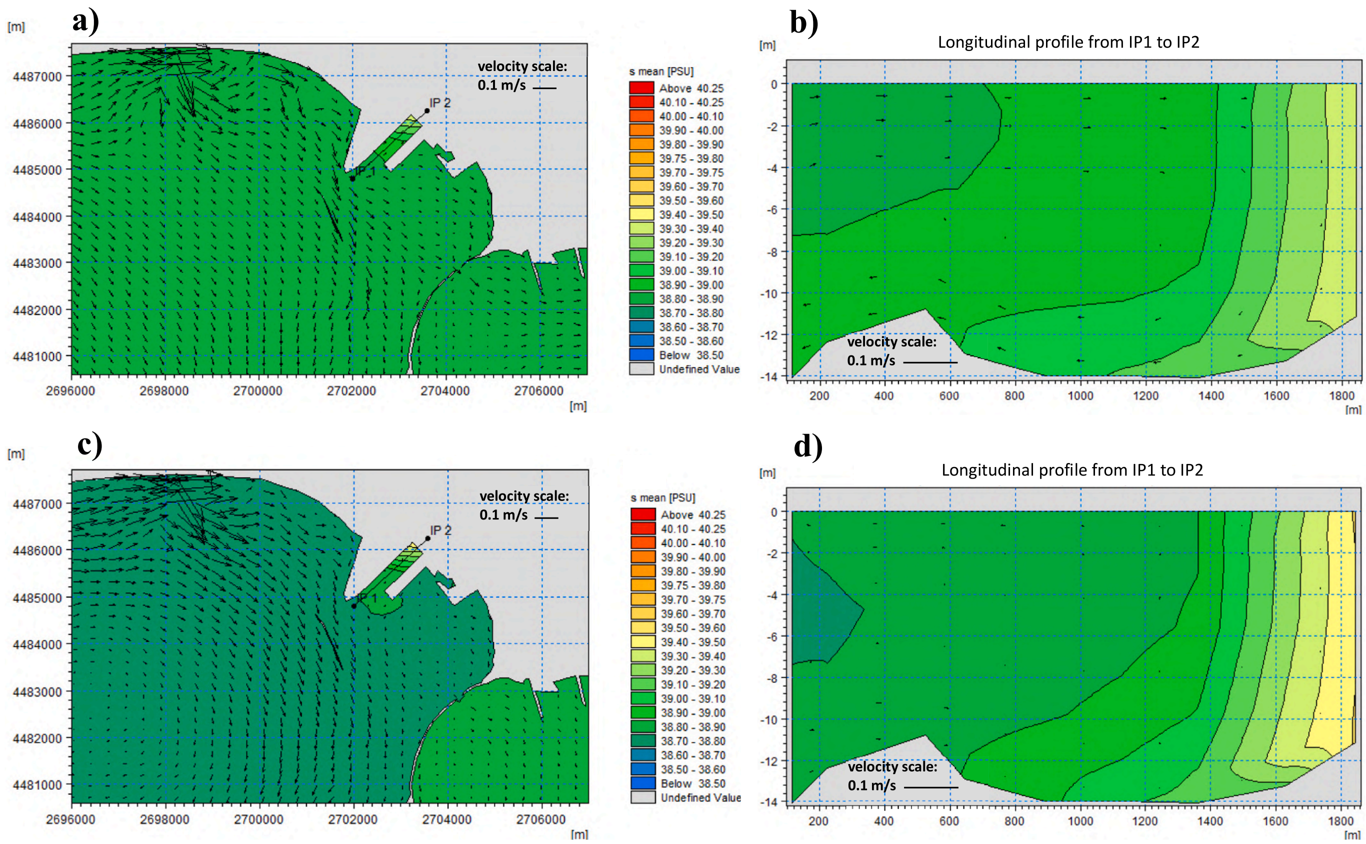

Fig. 8. Test HS2, time-averaged velocity maps. Left column: horizontal surface layer; Gaus Boaga Coordinates. Right column: selected vertical section along the inlet (IP1 – IP2). Top row: winter season; Bottom row: summer season.

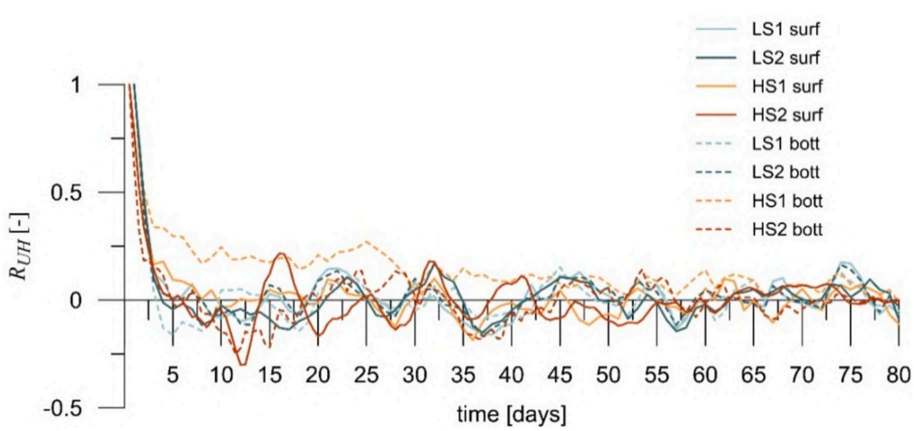

Fig. 9. Autocorrelation function of surface and bottom velocity, at the midpoint of the longitudinal transect IP1-IP2 of the inlet, for both LS tests and HS tests.

Smagorinsky formulation to calculate the horizontal eddy viscosity. This, in turn, determines the horizontal diffusivity K_H through the Prandtl number (assumed to be 1 in the model). In any way, we can get K_H also by multipling the integral time scale τ_H by the time-averaged variance of the velocity u_H, in the horizontal plane [26,28]. In Fig. 10, referring to the surface as an example, the trend of K_H along the longitudinal axis of the inlet (IP1-IP2) is shown. It is evident that, throughout the entire inlet, K_H is higher at each point in both LS cases compared to the HS cases, or at least equal. Outside the inlet, in the larger domain where additional hydrodynamic factors come into play, the opposite occurs, with K_H values higher in the HS tests. The values of K_H have order of magnitude O(10^4-10^6 cm^2/s) consistent with those deduced in other field surveys [26,29,30]. The trend of Fig. 10 further justifies the faster spreading at surface of the negatively buoyant plume within the inlet. Consequently, K_H diffusivity serves as a valuable indicator of environmental status. Once the plume exits the inlet, the diffusivity is initially dampened but then increases again as particles become trapped by the circulation structures established in the larger domain.

4.4. Open sea release of the hypersaline plume

In Test HS3, we evaluate the case in which the 50 psu hypersaline plume, rather than being discharged within the inlet, is instead conveyed offshore via a bottom submarine pipe terminating with a diffuser. The diffuser outlet is located approximately 3 km from the coastline, along the inlet's main axis, at 40.48° N, 17.13° E (that is

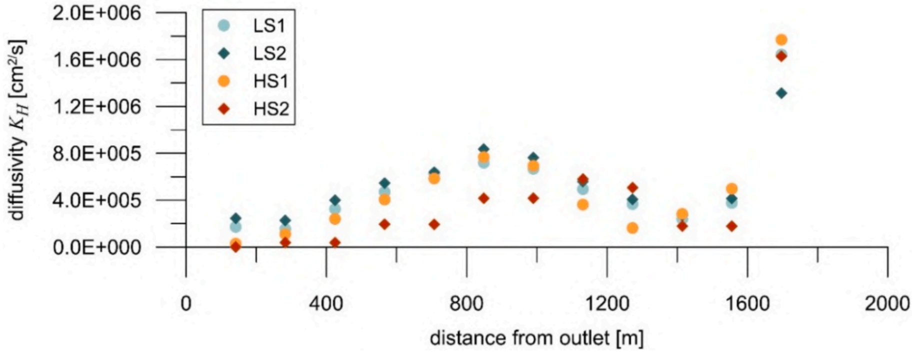

Fig. 10. Trend of surface horizontal diffusivity along the longitudinal transect IP1-IP2 of the inlet.

2,700,200 m E, 4483500 m N in Gauss-Boaga coordinates), where the water depth is roughly 20 m (Fig. 11). Technical constraints on system installation are beyond our scope; here, we focus on how this offshore release alters plume spreading compared to the inlet point release. Thus, Fig. 11 presents horizontal salinity maps for average winter conditions at the bottom (a) and surface (b), and for average summer conditions at the bottom (c) and surface (d).

In the winter case, currents at this offshore release site exhibit higher velocities than those within the inlet. Consequently, plume mixing and dispersion occur more rapidly and intensely, remaining confined to a relatively small area. For instance, Fig. 11a shows that, near the bottom, salinity slightly exceeds ambient values, with a maximum increase of approximately 0.5 % psu over an area of less than 1 km^2. A similar weak anomaly is evident at the surface (Fig. 11b). Overall, the localized salinity excess appears to be quickly incorporated into the broader background pattern of increasing salinity observed along the southeast-to-northwest axis of the domain.

In the summer case, bottom salinity near the diffuser reaches about 38.8 psu (a relative increase close to 0.8 %), which remains comparable to background values at the entrance to the Mar Grande basin (Fig. 11c). Although the salinity increase is minimal, the affected area at bottom is more extensive in summer than in winter and stretches toward the northern part of the domain. From bottom to surface, the plume's influence diminishes progressively (Fig. 11d).

It should be noted that the salinity scale in Fig. 11 is intentionally adjusted to enhance plume visibility and emphasize seasonal patterns. Accordingly, it differs from the scale adopted in Figs. 5–8, where the minimal salinity variations would otherwise be scarcely detectable. In fact, compared with Tests HS1 and HS2, Test HS3 produces lower salinity anomalies near the release point throughout the entire modelled period, and, as expected, the inlet remains completely unaffected. Therefore, if technically and economically feasible, this offshore release strategy could serve as a valid alternative to inlet discharge of a hyeprsaline plume, enabling its rapid mixing and dilution without significantly impacting the coastal environment. Specifically, for Test HS3 the computed macro-timescales (at a distance from the discharge comparable to that considered in the inlet release cases) are approximately 26 h at the bottom and 23 h at the surface, while the horizontal diffusivity is on the order of 10^6 cm^2/s at both surface and bottom.

5. Discussion

Roberts et al. [31] suggested that using groundwater desalination could be a more sustainable alternative to seawater desalination, though its feasibility depends on the availability of suitable groundwater resources. One key advantage is the potential reduction in energy costs, along with the discharge of water that has a lower salinity than seawater. While lower energy consumption is a clear benefit, the release of brackish water into marine environments raises new environmental concerns, shifting the focus from hypersaline brines to hyposaline effluents [32]. To explore this issue, we conducted numerical simulations using the MIKE 3FM model [18]. After validating the model with field data, we simulated four different scenarios in a target domain of the Ionian Sea maintaining the same boundary and initial conditions but varying the salinity of the discharged flow. Specifically, we examined both hypersaline (HS tests) and hyposaline (LS tests) effluents, considering surface and bottom release configurations within a coastal inlet, in accordance with stakeholder requirements, and assessed their respective impacts on hydrodynamics and, by extension, on the marine ecosystem. For completeness and comparison, we also included a scenario involving the release of hypersaline water in offshore conditions via a submarine pipeline equipped with a terminal diffuser. The following important aspects have emerged in terms of ecological and management implications, which can be extended to a broader and more general context, beyond the specifics of our local application.

5.1. *Salinity as a key variable for ecosystem health*

Salinity is a fundamental environmental factor shaping marine ecosystems, influencing species distribution, physiological processes, and ecosystem dynamics across all trophic levels [33,34]. Changes in salinity (whether due to climate change, freshwater input, or anthropogenic activities such as desalination discharges) can drive significant ecological shifts in both coastal and open-ocean systems. Coastal ecosystems, in particular, are highly sensitive to even minor salinity fluctuations, especially in times of climate change. In fact, climate change is amplifying salinity extremes: freshwater-dominated regions are becoming fresher, while high-salinity regions are becoming saltier due to changes in precipitation, evaporation, and circulation patterns [34,35]. These shifts are particularly pronounced in coastal areas, where complex land-sea interactions influence salinity dynamics, potentially forcing species to relocate while favoring more adaptable or tolerant organisms and disadvantaging others [34].

Our findings highlight the ecological implications of both hypersaline (HS tests) and hyposaline (LS tests) discharges, as they alter local hydrodynamics and, consequently, ecosystem functioning. Additionally, interactions between plume density and hydrodynamics can influence sediment transport, resuspension, and deposition, directly impacting benthic habitats, nutrient cycling, and associated organisms.

Referring to the release within the inlet, our results indicate that during summer, when water column stratification is strongest, hypersaline discharges intensify stagnation by reinforcing stratification, reducing vertical mixing, and exacerbating oxygen depletion in bottom waters [26]. This process could be particularly harmful to benthic communities, including key species such as crustaceans and mollusks, which play essential roles in nutrient cycling and food web stability. Bivalves are highly susceptible to salinity increases because of their low mobility and narrow physiological tolerance. The combination of elevated salinity and low oxygen availability creates stressful conditions that can lead to habitat degradation, reduced biodiversity, and shifts in

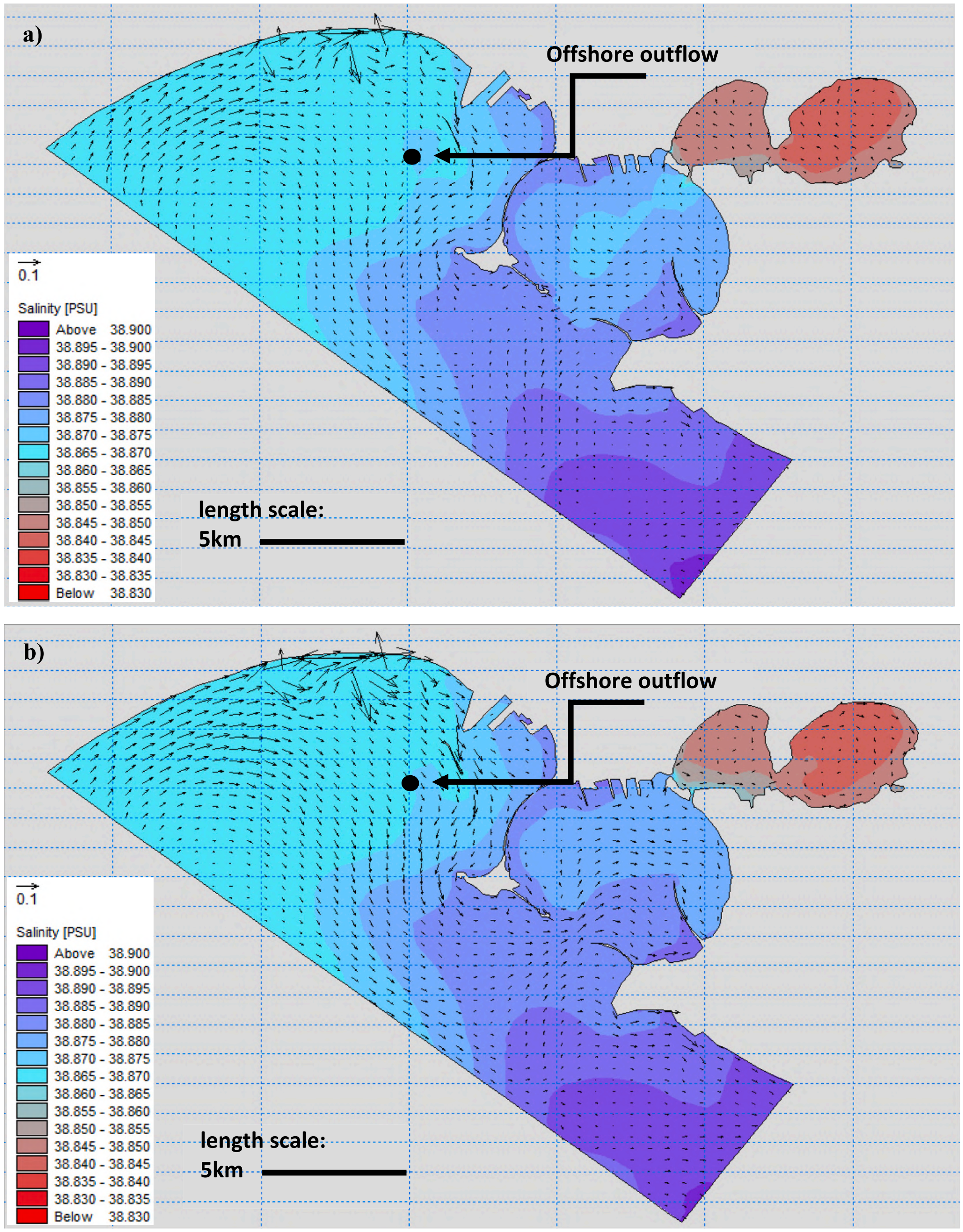

Fig. 11. Test HS3: Average horizontal maps of salinity and currents: (a) bottom layer, winter case; (b) surface layer, winter case; (c) bottom layer, summer case; (d) surface layer, summer case.

community composition, even altering population dynamics and local fisheries [36]. Fish larvae and juveniles could also be at risk, as even moderate salinity elevations, such as those caused by hypersaline discharges, can impair development and increase mortality due to their limited osmoregulatory capacity during early life stages. On the contrary, euryhaline benthic invertebrates and estuarine polychaetes tolerate salinity drops, often using low-salinity areas as nurseries and expanding their range [37].

Seagrass meadows, marsh grasses, and mangrove ecosystems are especially vulnerable to salinity fluctuations. Green algae like *Ulva Lactuca*. and seagrasses such as *Ruppia cirrhosa* thrive in low-salinity conditions while other seagrass species can tolerate short-term salinity changes. The Mediterranean seagrass *Posidonia oceanica* serves as a key bioindicator of environmental change, being especially vulnerable to both increased and reduced salinity. These fluctuations can cause physiological stress and lead to dieback, particularly if the plants are already under pressure from pollution and climate change [38].

Coral distribution and health are also affected by salinity shifts. Corals generally tolerate high salinity and may even show reduced bleaching susceptibility under such conditions [39], whereas lower salinity has more detrimental effects by reducing respiration and photosynthetic rates. Overall, we can remark that although isolated salinity shifts may not be the primary driver of ecosystem decline, they can contribute to functional impairment, particularly when combined

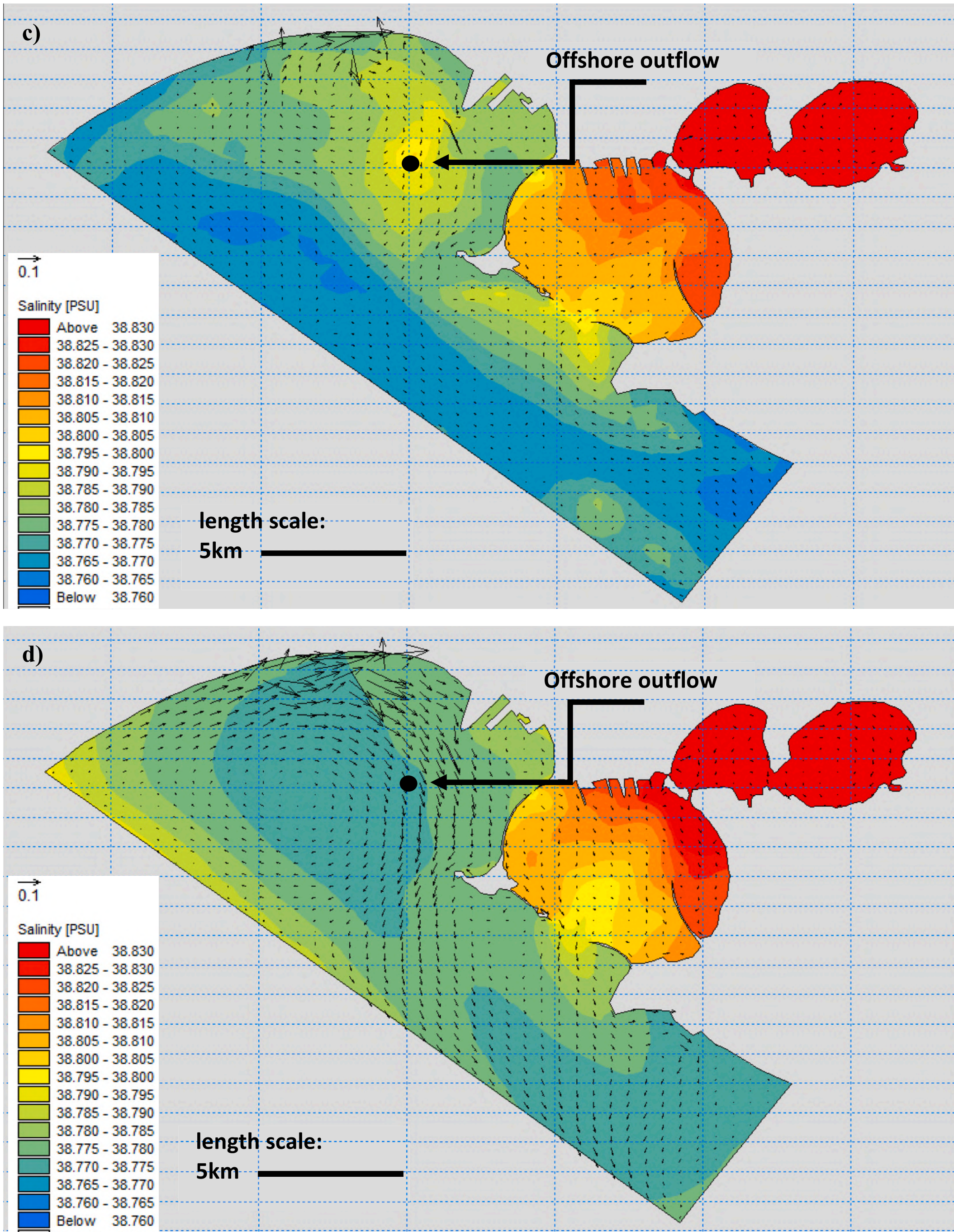

Fig. 11. (*continued*).

with other stressors such as ocean warming and acidification [40].

If we now consider the values obtained for the indicators K_H and τ_H in both the hypersaline and brackish discharge scenarios, the following can be deduced. Taking into account possible tolerance thresholds, it is generally recognized that a salinity deviation of up to 5 psu from ambient conditions can be tolerated by benthic communities, provided that horizontal mixing is sufficiently high ($K_H > 10^4$ cm^2/s) and exposure durations are short ($\tau_H < 48$ h), thereby preventing prolonged physiological stress [36,37]. Based on these criteria, Test HS3 can be considered the most environmentally neutral solution, posing virtually no significant ecological risk. Among the inlet release scenarios, developed in response to stakeholder input, Test LS2 emerges as the option with the lowest overall impact on the ecosystem.

5.2. *Implications for coastal management*

It is evident that if coastal ecosystems, which provide essential services vital for human well-being, are negatively impacted by desalination plant effluents, their degradation will result not only in environmental loss but also in significant economic consequences [41].

Thus, the ecological risks associated with both hyposaline and hypersaline discharges highlight the need for effective management strategies to balance desalination needs with ecological sustainability.

In order to minimize the ecological effects in the near field, traditional desalination plant outfalls have been designed to optimize mixing and dilution of the brine with the ambient waters (e.g., using approaches such as diffusers or pre-mixing with power-plant cooling water), to promote a rapid reduction of salinity excess in the immediate discharge area [42]. However, our findings for HS case indicate that hypersaline discharge may exacerbate stratification and consequently stagnation, leading to localized hotspots of environmental stress. For example, enhanced stratification could inhibit nutrient exchange and reduce productivity, directly affecting ecosystem services such as fisheries and aquaculture. In contrast, the discharge of brackish waters (LS cases) appears to promote more water mixing and mitigate stagnation risks, helping sustain ecosystem services and biodiversity, particularly during summer months when marine ecosystems are already under stress.

Certainly, along with the need to minimize localized salinity extremes, additional management actions are necessary and can be summarized in two key tasks: i) monitoring and regularly tracking salinity, currents, and ecological indicators especially in sensitive habitats, such as seagrass meadows or coral reefs, to detect early signs of stress and emerging hotspots [9]; ii) integrating climate adaptation strategies in marine spatial planning, that is accounting for projected salinity shifts for developing effective conservation strategies, taking into account seasonal and climatic variability.

Regarding the first task, monitoring programs can be designed to track the proposed metrics in real time, and adaptive management thresholds can be set accordingly. Because both indicators K_H and τ_H derive from routinely measured salinity and flow data, our framework is readily transferable to other coastal desalination sites. Moreover, monitoring should extend beyond the discharge from desalination processes to include the groundwater systems from which water is extracted. In our case, it is equally important to assess the characteristics of the aquifer feeding the Tara spring system. This system lies in a geologically complex area with two aquifers: a shallow one in terraced marine deposits and a deeper, artesian one in Cretaceous carbonates. The latter, which feeds the spring, is overlain by clay layers and floats above intruding seawater, leading to salinity stratification [17]. Salinity variations depend on the balance between the freshwater lens and seawater intrusion, highlighting the need for detailed hydrogeological studies and long-term monitoring, especially in light of climate change impacts on sea level and groundwater quality. We would like to clarify that no additional water extraction beyond existing conditions is required to supply the proposed plant. No increased exploitation of the aquifer is anticipated compared to the current situation. The Tara system today, including the main spring and several smaller springs, already provides a volume that naturally discharges at the surface, sufficient to supply the total flow rate necessary for the plant.

By proactively addressing these challenges, we can help maintain the ecological integrity of coastal and marine systems while balancing the growing demand for desalinated water alongside other anthropogenic modifications to the coastal environment.

6. Conclusion

In this study, we analyzed the potential impacts of discharging hyposaline effluent, rather than traditional brine, from a desalination plant located in a highly vulnerable coastal area. Using a numerical model, we investigated four scenarios involving discharges within an inlet: hyposaline water released at the bottom (Test LS1), hyposaline water released at the surface (Test LS2), hypersaline water released at the bottom (Test HS1), and hypersaline water released at the surface (Test HS2). An additional scenario (Test HS3) considered the discharge of hypersaline water into the open sea via a submarine pipeline with a diffuser.

For inlet releases, the results show that plume salinity significantly influences local hydrodynamics. In particular, hypersaline discharges intensify stagnation, reinforce summer stratification, and reduce water renewal, especially near the bottom during warmer months. By contrast, in the offshore release scenario (Test HS3), the hypersaline plume's effect is minimal: rapid mixing and dispersion driven by local bottom currents limit salinity increases to 0.5 % in winter and 0.8 % in summer, relative to ambient conditions. These results suggest that, where feasible, offshore diffuser systems should be prioritized for hypersaline discharges.

This findings are further supported by two ecologically relevant metrics, i.e. the horizontal eddy diffusivity K_H and the macro time scale τ_H, used to assess the impact of desalination plumes on marine habitats. Their simplicity, based on commonly available field measurements, makes them practical tools for integrated monitoring and management. This indicator-based approach provide a consistent and transferable method for evaluating discharge impacts across diverse coastal settings.

Given the central role of salinity in shaping marine ecosystems, particularly under climate change, its variability must be closely monitored and considered in marine spatial planning. This study underscores the importance of numerical modeling for evaluating discharge scenarios and guiding environmentally sound design choices. Integrating model-based insights into regional management plans can help mitigate ecological impacts. Future research should prioritize long-term monitoring to assess the combined effects of desalination and climate change, and to define ecological thresholds of tolerance.

CRediT authorship contribution statement

Francesca De Serio: Writing – review & editing, Writing – original draft, Methodology, Investigation, Formal analysis, Conceptualization. **Diana De Padova:** Writing – review & editing, Formal analysis. **Giancarlo Chiaia:** Writing – review & editing, Methodology, Conceptualization. **Mouldi Ben Meftah:** Writing – review & editing. **Michele Mossa:** Writing – review & editing.

Declaration of competing interest

The authors declare that they have no known competing financial interests or personal relationships that could have appeared to influence the work reported in this paper.

Data availability

Data will be made available on request.

References

[1] S. Soni, M.K. Jindal, P.K. Tewari, V. Anand, Potential and challenges of desalination technologies for arid and semiarid regions: a comprehensive review, Desalination 600 (2025), https://doi.org/10.1016/j.desal.2024.118458.

[2] A. Panagopoulos, A comparative study on minimum and actual energy consumption for the treatment of desalination brine, Energy 212 (2020) 118733, https://doi.org/10.1016/j.energy.2020.118733.

[3] R. Sirota, G. Winters, O. Levy, J. Marques, A. Paytan, J. Silverman, G. Sisma-Ventura, E. Rahav, G. Antler, E. Bar-Zeev, Impacts of desalination brine discharge on benthic ecosystems, Environ. Sci. Technol. 58 (2024) 5631–5645, https://doi.org/10.1021/acs.est.3c07748.

[4] M. Ayaz, M.A. Namazi, M.A. ud Din, M.I.M. Ershath, A. Mansour, el-H.M. Aggoune, Sustainable seawater desalination: current status, environmental implications and future expectations, Desalination 540 (2022) 116022, https://doi.org/10.1016/j.desal.2022.116022.

[5] Y. Fernández-Torquemada, J.M. Gónzalez-Correa, A. Loya, L.M. Ferrero, M. Díaz-Valdés, J.L. Sánchez-Lizaso, Dispersion of brine discharge from seawater reverse osmosis desalination plants, Desalin. Water Treat. 5 (2009) 137–145, https://doi.org/10.5004/dwt.2009.576.

[6] D. Malcangio, A.F. Petrillo, Modeling of brine outfall at the planning stage of desalination plants, Desalination 254 (2010) 114–125, https://doi.org/10.1016/j.desal.2009.12.005.

[7] A. Purnama, D. Shao, Modeling brine discharge dispersion from two adjacent desalination outfalls in coastal waters, Desalination 362 (2015) 68–73, https://doi.org/10.1016/j.desal.2015.02.012.

[8] M. Amitouche, A. Lefkir, B. Remini, M.S. Sebki, L. Aissaoui, Diagnosis and improvement of diffuser performance of Fouka desalination plant (Algeria), Desalin. Water Treat. 255 (2022) 94–100, https://doi.org/10.5004/dwt.2022.28325.

[9] Y. Fernández-Torquemada, A. Carratalá, J.L.S. Lizaso, Impact of brine on the marine environment and how it can be reduced, Desalin. Water Treat. 167 (2019) 27–37, https://doi.org/10.5004/dwt.2019.24615.

[10] M. Polemio, V. Dragone, P.P. Limoni, Monitoring and methods to analyse the groundwater quality degradation risk in coastal karstic aquifers (Apulia, southern

Italy), Environ. Geol. 58 (2009) 299–312, https://doi.org/10.1007/s00254-008-1582-8.
[11] F. De Serio, M. Mossa, Environmental monitoring in the mar Grande basin (Ionian Sea, southern Italy), Environ. Sci. Pollut. Res. 23 (2016) 12662–12674, https://doi.org/10.1007/s11356-015-4814-y.
[12] F. De Serio, E. Armenio, M. Ben Meftah, G. Capasso, V. Corbelli, D. De Padova, F. De Pascalis, A. Di Bernardino, G. Leuzzi, P. Monti, A. Pini, R. Velardo, M. Mossa, Detecting sensitive areas in confined shallow basins, Environ. Model. Software 126 (2020) 104659, https://doi.org/10.1016/j.envsoft.2020.104659.
[13] D. De Padova, M. Ben Meftah, F. De Serio, M. Mossa, Management of dredging activities in a highly vulnerable site: simulation modelling and monitoring activity, J. Mar. Sci. Eng. 8 (2020) 1020, https://doi.org/10.3390/jmse8121020.
[14] E. Armenio, F. De Serio, M. Mossa, Analysis of data characterizing tide and current fluxes in coastal basins, Hydrol. Earth Syst. Sci. 21 (2017) 3441–3454, https://doi.org/10.5194/hess-21-3441-2017.
[15] G. Chimienti, D. De Padova, M. Adamo, M. Mossa, A. Bottalico, A. Lisco, N. Ungaro, F. Mastrototaro, Effects of global warming on Mediterranean coral forests, Sci. Rep. 11 (2021) 20703, https://doi.org/10.1038/s41598-021-00162-4.
[16] A. Galeandro, A. Doglioni, V. Simeone, Success of reclamation works and effects of climatic changes in Taranto area: South Italy, in: Engineering Geology for Society and Territory - Volume 1, Springer International Publishing, Cham, 2015, pp. 165–168, https://doi.org/10.1007/978-3-319-09300-0_31.
[17] V. Cotecchia, Le acque sotterranee e l'intrusione marina in Puglia: dalla ricerca all'emergenza nella salvaguardia della risorsa, in: Memorie descrittive della Carta Geologica d'Italia, ISPRA Serv. Geologico d'Italia, 92, 2014 (in Italian).
[18] A. Feola, I. Lisi, A. Salmeri, F. Venti, A. Pedroncini, M. Gabellini, E. Romano, Platform of integrated tools to support environmental studies and management of dredging activities, J. Environ. Manage. 166 (2016) 357–373, https://doi.org/10.1016/j.jenvman.2015.10.022.
[19] R. Escudier, E. Clementi, A. Cipollone, J. Pistoia, M. Drudi, A. Grandi, V. Lyubartsev, R. Lecci, A. Aydogdu, D. Delrosso, M. Omar, S. Masina, G. Coppini, N. Pinardi, A high resolution reanalysis for the Mediterranean Sea, Front. Earth Sci. 9 (2021), https://doi.org/10.3389/feart.2021.702285.
[20] W. Rodi, Examples of calculation methods for flow and mixing in stratified fluids, J. Geophys. Res. Oceans 92 (1987) 5305–5328, https://doi.org/10.1029/JC092iC05p05305.
[21] J. Smagorinsky, Large eddy simulation of complex engineering and geophysical flows, in: B. Galperin, S.A. Orszag (Eds.), Evolution of Physical Oceanography, Cambridge University Press, 1993, pp. 3–36.
[22] I. Petrosillo, A.M. Scardia Scardia, N. Ungaro, A. Specchiulli, G. Fanelli, G. Centoducati, F. De Serio, R. Carlucci, D. Valente, E. Barbone, A. Pini, C. G. Giannuzzi, T. Scirocco, E.M. Lovello, M. Deflorio, A.O. Lillo, D. De Padova, L. Papa, E. Goffredo, M.E. Mancini, M. Mossa, Towards sustainable marine spatial planning of aquaculture, Ecol. Indic. 154 (2023) 110542, https://doi.org/10.1016/j.ecolind.2023.110542.
[23] M. Mossa, E. Armenio, M. Ben Meftah, M.F. Bruno, De D. Padova, De F. Serio, Meteorological and hydrodynamic data in the mar Grande and mar Piccolo, Italy, of the coastal engineering laboratory (LIC) survey, winter and summer 2015, Earth Syst. Sci. Data 13 (2021) 599–607, https://doi.org/10.5194/essd-13-599-2021.
[24] D. Bouffard, T. Doda, C.L. Ramón, H.N. Ulloa, Thermally driven cross-shore flows in stratified basins: a review on the thermal siphon dynamics, Flow 5 (2025) E1, https://doi.org/10.1017/flo.2024.31.
[25] M. De Dominicis, G. Leuzzi, P. Monti, N. Pinardi, P.-M. Poulain, Eddy diffusivity derived from drifter data for dispersion model applications, Ocean Dyn. 62 (2012) 1381–1398, https://doi.org/10.1007/s10236-012-0564-2.
[26] F. De Serio, D. De Padova, M. Ben Meftah, M. Mossa, A framework for data analysis from long-term monitoring in anthropized coastal areas, J. Ecohydraul. (2024) 1–23, https://doi.org/10.1080/24705357.2024.2428959.
[27] A. Di Bernardino, P. Monti, G. Leuzzi, G. Querzoli, Eulerian and Lagrangian time scales of the turbulence above staggered arrays of cubical obstacles, Environ. Fluid Mech. 20 (2020) 987–1005, https://doi.org/10.1007/s10652-020-09736-8.
[28] M.G. Gaeta, A.G. Samaras, R. Archetti, Numerical investigation of thermal discharge to coastal areas: a case study in South Italy, Environ. Model. Software 124 (2020) 104596, https://doi.org/10.1016/j.envsoft.2019.104596.
[29] J. Chenoweth, R.A. Al-Masri, Cumulative effects of large-scale desalination on the salinity of semi-enclosed seas, Desalination 526 (2022) 115522, https://doi.org/10.1016/j.desal.2021.115522.
[30] A. Romanou, G. Tselioudis, C.S. Zerefos, C.-A. Clayson, J.A. Curry, A. Andersson, Evaporation–precipitation variability over the Mediterranean and the black seas from satellite and reanalysis estimates, J. Climate 23 (2010) 5268–5287, https://doi.org/10.1175/2010JCLI3525.1.
[31] D.A. Roberts, E.L. Johnston, N.A. Knott, Impacts of desalination plant discharges on the marine environment: a critical review of published studies, Water Res. 44 (2010) 5117–5128, https://doi.org/10.1016/j.watres.2010.04.036.
[32] T. Röthig, S.M. Trevathan-Tackett, C.R. Voolstra, C. Ross, S. Chaffron, P.J. Durack, L.M. Warmuth, M. Sweet, Human-induced salinity changes impact marine organisms and ecosystems, Glob. Chang. Biol. 29 (2023) 4731–4749, https://doi.org/10.1111/gcb.16859.
[33] P.J. Durack, S.E. Wijffels, Fifty-year trends in global ocean salinities and their relationship to broad-scale warming, J. Climate 23 (2010) 4342–4362, https://doi.org/10.1175/2010JCLI3377.1.
[34] P.J. Durack, S.E. Wijffels, R.J. Matear, Ocean salinities reveal strong global water cycle intensification during 1950 to 2000, Science 336 (2012) 455–458, https://doi.org/10.1126/science.1212222.
[35] J. Velasco, C. Gutiérrez-Cánovas, M. Botella-Cruz, D. Sánchez-Fernández, P. Arribas, J.A. Carbonell, A. Millán, S. Pallarés, Effects of salinity changes on aquatic organisms in a multiple stressor context, Philos. Trans. R. Soc. Lond. B Biol. Sci. 374 (2019) 20180011, https://doi.org/10.1098/rstb.2018.0011.
[36] J.M. Sandoval-Gil, J.M. Ruiz, L. Marín-Guirao, Advances in understanding multilevel responses of seagrasses to hypersalinity, Mar. Environ. Res. 183 (2023) 105809, https://doi.org/10.1016/j.marenvres.2022.105809.
[37] R.H. Walker, A.C. Belvin, J.B. Mouser, A. Pennino, S. Plont, C.D. Robinson, L. B. Smith, J. Thapa, C.E. Zipper, P.L. Angermeier, S.A. Entrekin, Global review reveals how disparate study motivations, analytical designs, and focal ions limit understanding of salinization effects on freshwater animals, Sci. Total Environ. 892 (2023) 164061, https://doi.org/10.1016/j.scitotenv.2023.164061.
[38] C. D'Angelo, J. Wiedenmann, Impacts of nutrient enrichment on coral reefs: new perspectives and implications for coastal management and reef survival, Curr. Opin. Environ. Sustain. 7 (2014) 82–93, https://doi.org/10.1016/j.cosust.2013.11.029.
[39] Intergovernmental Panel on Climate Change (IPCC), Climate Change 2021 – The Physical Science Basis: Working Group I Contribution to the Sixth Assessment Report of the Intergovernmental Panel on Climate Change, Cambridge University Press, 2023, https://doi.org/10.1017/9781009157896.002.
[40] R. Costanza, R. d'Arge, R. de Groot, S. Farber, M. Grasso, B. Hannon, K. Limburg, S. Naeem, R.V. O'Neill, J. Paruelo, R.G. Raskin, P. Sutton, M. van den Belt, The value of the world's ecosystem services and natural capital, Nature 387 (1997) 253–260, https://doi.org/10.1038/387253a0.
[41] M.A. Young, O. Serrano, P.I. Macreadie, C.E. Lovelock, P. Carnell, D. Ierodiaconou, National scale predictions of contemporary and future blue carbon storage, Sci. Total Environ. 800 (2021) 149573, https://doi.org/10.1016/j.scitotenv.2021.149573.
[42] T. Bleninger, G.H. Jirka, Modelling and environmentally sound management of brine discharges from desalination plants, Desalination 221 (2008) 585–597, https://doi.org/10.1016/j.desal.2007.02.059.